ELASTIC BODY SPLINE BASED IMAGE SEGMENTATION

Sachin Meena[⋆] *V. B. Surya Prasath*[⋆] *Kannappan Palaniappan*[⋆] *Guna Seetharaman*[†]

[⋆]Department of Computer Science, University of Missouri-Columbia, MO 65211 USA
[†]Air Force Research Laboratory, Rome, NY 13441 USA

ABSTRACT

Elastic body splines (EBS) belonging to the family of 3D splines were recently introduced to capture tissue deformations within a physical model-based approach for non-rigid biomedical image registration [1]. EBS model the displacement of points in a 3D homogeneous isotropic elastic body subject to forces. We propose a novel extension of using elastic body splines for learning driven figure-ground segmentation. The task of interactive image segmentation, with user provided foreground-background labeled seeds or samples, is formulated as learning an interpolating pixel classification function that is then used to assign labels for all unlabeled pixels in the image. The spline function we chose to model the supervised pixel classifier is the Gaussian elastic body spline (GEBS) which can use sparse scribbles from the user and has a closed form solution enabling a fast on-line implementation. Experimental results demonstrate the applicability of the GEBS approach for image segmentation. The GEBS method for interactive foreground image labeling shows promise and outperforms a previous approach using the thin-plate spline model.

Index Terms— Interactive image segmentation, supervised regression, elastic body, 3D splines.

1. INTRODUCTION

Interactive figure-ground segmentation has become very popular in recent years as it overcomes some of the inherent problems associated with unsupervised image segmentation where weak boundaries, textured regions, similar intensity levels in the foreground and background make the image segmentation problem ill-posed. A large number of user guided image segmentation algorithms have been developed over the past two decades ranging from marking boundary pixels [2, 3], initializing a contour close to the region of interest [4, 5], drawing a box around the object [6] or placing some seeds or scribbles on the desired object and its background [7]. Interactive semi-supervised segmentation can improve automatic algorithms for high-throughput scalable applications where high accuracy is required but failure modes are many.

Automatic image segmentation approaches are highly susceptible to initial conditions, parameter values, weak boundaries and noise. We review a few popular methods.

(a) Input with seeds (b) Our GEBS result (c) TPS [8]

Fig. 1. Sparse user-defined seed points or interactive scribbles shown in (a) provide 14 labeled samples for the Gaussian Elastic Body Spline (GEBS) algorithm that produces a more accurate segmentation shown in (b) compared to the thin-spline regression-based segmentation [8] results shown in (c). The interactive user input points sparsely sampling the foreground and background are just single pixels but shown as thick dots for ease of visibility.

Snakes and active contour deformable models [4, 9] need the user or algorithm to initialize a curve close to the desired object boundary and the curve is evolved under forces derived from edge [4] or region information [9]. Main limitations of these methods are that the energy functions are non-convex in nature and therefore the final contours are only a local optimum; also these evolved contours being initialization dependent are greatly affected by the initial input provided by the user. Interactive graph-based approaches [10] solve the image segmentation problem using min/max network flow methods and in [11] they add a geodesic star-convexity shape constraint to the energy minimization. Graph cut based techniques often suffer from the problem of over-segmentation since they produce "short cuts" for the optimal solution.

Our experience has been that fast user-guided image segmentation methods would be very helpful for segmentation and tracking applications [12, 13, 14, 15] where subject matter experts can provide interactive guidance to improve the performance of automatic or semi-automatic algorithms, but that the amount of user-interaction needs to be reduced for effective systems [16, 17]. In lazy snapping [18], live-wire [3] and intelligent scissors [2] the user provides as input some initial boundary information which is then used to complete the image segmentation task. We refer to [19] for a comprehensive review covering many interactive image segmentation methods to date and their performance. Although many interactive image segmentation systems have been developed there is a need for reducing user input, increased robustness to noise and better detection of weak object boundaries.

In order to address these limitations we develop a framework for interactive image segmentation based on interpolating spline functions that with very few user (scribble) inputs produces high quality segmentations. We propose using Gaussian Elastic Body Splines (GEBS) for regression-based pixel classification with sparse user-defined seed points that are used to interpolate seed point labels for the remaining unlabeled pixels in the image. Our method is similar to the spline based image segmentation method studied in [8] which is based on thin-plate splines [20]. Both methods make use of the interpolating property of (multivariate) splines to learn a pixel classification operator and solve similar systems of linear equations to obtain the coefficients for the interpolating spline classifier functions. However there are two fundamental differences between the two approaches: (a) The underlying partial differential equation (PDE) solutions used in the two methods are derived differently. The GEBS are analytic solutions of the Navier equilibrium PDE, while thin plate splines solve the biharmonic equation $\Delta^2 f = 0$. (b) The spline functions used in [8] are radial basis functions of the form $r^2 \log r$, whereas our method makes use of Gaussian functions. Our proposed method is able to obtain good results even from a sparse quickly defined set of user-provided labels (input seeds), in comparison to the thin-plate spline regression results of [8] (see Figure 1). Using sparse input seeds and solving only a linear system of equations to learn the spline coefficients makes our algorithm easy to implement and fast enough for on-line use. We provide comparative image segmentation results on natural images and the results indicate GEBS provides a clear improvement over thin plate splines.

The rest of the paper is organized as follows. In Section 2 we provide a brief description of the EBS based image registration method, and its adaptation for interactive image segmentation with the relevant mathematical framework. In Section 3 we provide segmentation results using the proposed method followed by conclusions in Section 4.

2. GEBS FOR IMAGE SEGMENTATION

2.1. Elastic Body Splines

Non-rigid registration and deformable modeling approaches have been used to model natural phenomena [21, 22]. Elastic body splines (EBS) belong to the class of 3D splines suggested by Davis et al [20] and mainly used for elastic registration of biomedical images. Given the displacement for landmark points $\vec{p}_i$, $i = 0, \ldots, N$ between source and target images a transformation is determined that maps the corresponding landmarks from the source to the target image and interpolates the displacement field for all the remaining points in the transformed image. The transformation is given as,

$$\vec{d}(\vec{x}) = \mathbf{A}\vec{x} + \vec{b} + \sum_{i=0}^{N} \mathbf{G}(\vec{x} - \vec{p}_i)\vec{c}_i. \tag{1}$$

where a linear affine transformation is combined with non-linear elastic transformations $\mathbf{G}(\vec{x} - \vec{p}_i)\vec{c}_i$ to obtain the displacement field. Here $\mathbf{G}$ is the spline function, $\vec{d}(\vec{x})$ is the displacement vector for the landmark points, $\vec{p}_i$, $\mathbf{A}$ and $\vec{b}$ are the coefficients for the affine transformation and $\vec{c}_i$ the set of coefficients for the non-linear elastic terms.

We note that the physical model used for the EBS Navier equilibrium PDE is given by,

$$\mu\nabla^2\vec{u}(\vec{x}) + (\mu + \lambda)\nabla[\nabla \cdot \vec{u}(\vec{x})] = \vec{f}(\vec{x}), \tag{2}$$

which models the deformation of a homogeneous isotropic elastic body subjected to loads. Here $\vec{u}(\vec{x})$ is the displacement, $\vec{f}(\vec{x})$ the force field, μ, λ are the Lame coefficients, ∇^2, ∇ denote the Laplacian and gradient respectively. The solution of (2) is obtained by the Galerkin vector method [23]. By using this method three coupled PDEs for $\vec{u}(\vec{x})$ are transformed into three independent radially symmetric biharmonic PDEs. Davis *et al.* [20] used symmetric forces, however, these forces are singular at the origin and do not decrease as fast as the increase in distances between the landmark points; see [20] for more details. Kohlrausch *et al.* [1] have suggested that GEBS which use Gaussian forces supports the use of transformations modeling local (non-linear) deformations,

$$\vec{f}(\vec{x}) = \vec{c}_i \frac{1}{(\sqrt{2\pi}\sigma)^3} \exp \frac{-||\vec{x}||^2}{2\sigma^2}. \tag{3}$$

where $||\vec{x}||$ is the norm and σ is a scale parameter. An analytic solution for the PDE (2) with force field Eq. (3) is from [1],

$$\vec{u}(\vec{x}) = \frac{1}{16\pi S}\frac{1}{1-\nu}\mathbf{G}(\vec{x})\vec{c}, \tag{4}$$

where S is the shear modulus and ν the Poisson ratio,

$$\begin{aligned}\mathbf{G}(\vec{x}) = \Bigg[& \left((4(1-\nu)-1)\frac{\mathrm{Erf}(\hat{r})}{r} \right. \\ & \left. - \sqrt{\frac{2}{\pi}}\sigma\frac{e^{-\hat{r}^2}}{r^2} + \sigma^2\frac{\mathrm{Erf}(\hat{r})}{r^3} \right)\mathbf{I} \\ & + \left(\frac{\mathrm{Erf}(\hat{r})}{r^3} + 3\sqrt{\frac{2}{\pi}}\sigma\frac{e^{-\hat{r}^2}}{r^4} - 3\sigma^2\frac{\mathrm{Erf}(\hat{r})}{r^5} \right)\vec{x}\vec{x}^T \Bigg].\end{aligned} \tag{5}$$

Here $\mathrm{Erf}(\cdot)$ is the standard error function, $\hat{r} = |\vec{x}|/\sqrt{2}\sigma$, $\mathbf{I}$ is the identity matrix, $\vec{x}\vec{x}^T$ is an outer product. Note that for the transformation (1) we use $\mathbf{G}(\vec{x})$ given by (5).

2.2. New Framework for Interactive Image Segmentation

For an interactive image segmentation task we learn the interpolating pixel classification function $\vec{d}(\vec{x})$ in (1) from the user supplied seed points such that $\vec{d}(\vec{x}) = [+1 + 1 + 1]^T$ for foreground pixels and $\vec{d}(\vec{x}) = [-1 - 1 - 1]^T$ for background

(a) Input with seeds (b) Manual ground truth (BSDS500) (c) Our GEBS result (d) TPS [8]

Fig. 2. Comparison of segmentation results on three BSDS 500 images along with one manual ground-truth. Although the images are shown in color only gray scale intensities are used in the GEBS model. (a) Input image with user provided foreground (green) and background (red) seed points. (b) Sample human annotated ground truth. (c) Our GEBS segmentation results. (d) TPS segmentation results [8].

pixels. $\vec{x}$ is a feature vector comprised of spatial location and grayscale value of the pixel. Coefficients $\mathbf{A}$, $\vec{b}$, and $\vec{c}_i$ are computed using (1) from the seed points. Let $\mathbf{A}\vec{x}+\vec{b}$, be the affine part of the GEBS interpolating function,

$$\mathbf{A} = [\vec{a_1} \quad \vec{a_2} \quad \vec{a_3}]. \tag{6}$$

Let $\mathbf{W}$ be the vector of all the GEBS coefficients given as,

$$\mathbf{W} = \begin{bmatrix} \mathbf{C}_F & \mathbf{C}_B & \vec{a}_1^T & \vec{a}_2^T & \vec{a}_3^T & \vec{b}^T \end{bmatrix}^T \tag{7}$$

where $\mathbf{C}_F$ and $\mathbf{C}_B$ are the elastic coefficients corresponding to, f, foreground seed pixels and, b, background seed pixels,

$$\mathbf{C}_F = \begin{bmatrix} \vec{c}_1^T \dots \vec{c}_f^T \end{bmatrix}, \quad \mathbf{C}_B = \begin{bmatrix} \vec{c}_1^T \dots \vec{c}_b^T \end{bmatrix}.$$

The Gaussian Elastic Body Spline (GEBS) mapping determined by the weights $\mathbf{W}$ that we are solving for is given by the relationship, $\mathbf{Y} = \mathbf{LW}$, where $\mathbf{Y}$ is the set of displacement vectors for the user defined seeds. When matrix $\mathbf{L}$ is singular or close to being singular, computational techniques such as SVD can be used to obtain the GEBS coefficients. The GEBS coefficients are estimated by solving the matrix equation,

$$\mathbf{W} = \mathbf{L}^{-1}\mathbf{Y} \tag{8}$$

where,

$$\mathbf{L} = \begin{bmatrix} \mathbf{K} & \mathbf{P} \\ \mathbf{P}^T & \mathbf{O} \end{bmatrix}, \quad \mathbf{K} = \begin{bmatrix} \mathbf{G}_{FF} & \mathbf{G}_{FB} \\ \mathbf{G}_{BF} & \mathbf{G}_{BB} \end{bmatrix} \tag{9}$$

$$\mathbf{G}_{FF}(\vec{r}) = \begin{bmatrix} \mathbf{G}_{11}(\vec{r}_{11}) & \dots & \mathbf{G}_{1f}(\vec{r}_{1f}) \\ \vdots & & \vdots \\ \mathbf{G}_{f1}(\vec{r}_{11}) & \dots & \mathbf{G}_{ff}(\vec{r}_{ff}) \end{bmatrix} \tag{10}$$

with $\vec{r}_{ij} = \vec{x}_i - \vec{x}_j$ and $\vec{x}_i$ is the feature vector for the i^{th} foreground seed point. Hence, $\mathbf{G}_{FF}$ is the matrix of GEBS (5) functions defined only over foreground pixels. $\mathbf{G}_{FB}$, $\mathbf{G}_{BB}$ and $\mathbf{G}_{BF}$ are similarly defined,

$$\mathbf{P} = \begin{bmatrix} \mathbf{P}_F & \mathbf{I}_F \\ \mathbf{P}_B & \mathbf{I}_B \end{bmatrix}, \tag{11}$$

where the identity matrices are given by,

$$\mathbf{I}_F = \begin{bmatrix} \mathbf{I}_1 \dots \mathbf{I}_f \end{bmatrix}, \mathbf{I}_B = \begin{bmatrix} \mathbf{I}_1 \dots \mathbf{I}_b \end{bmatrix}, \mathbf{I} = \begin{bmatrix} 1 & 0 & 0 \\ 0 & 1 & 0 \\ 0 & 0 & 1 \end{bmatrix}, \tag{12}$$

for f foreground seed points, b background seed points and,

$$\mathbf{P}_F = \begin{bmatrix} x_{11}\mathbf{I} & x_{12}\mathbf{I} & x_{13}\mathbf{I} \\ \vdots & \vdots & \vdots \\ x_{f1}\mathbf{I} & x_{f2}\mathbf{I} & x_{f3}\mathbf{I} \end{bmatrix} \tag{13}$$

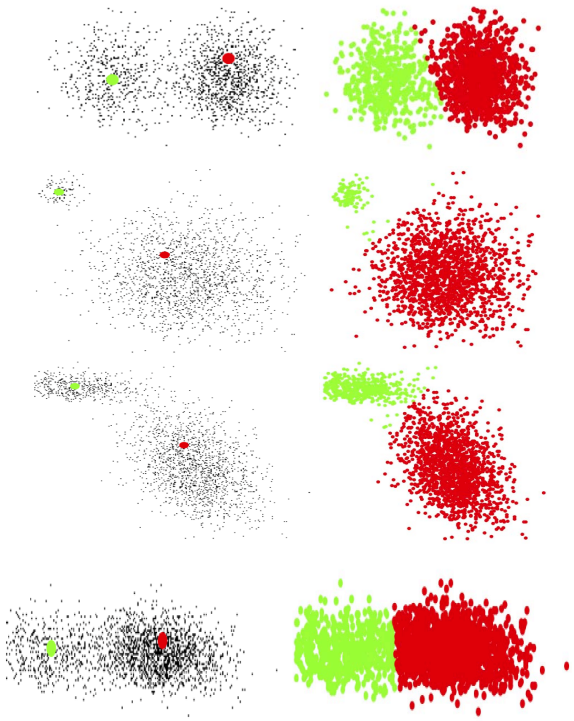

(a) Input with seeds (b) Our GEBS results

Fig. 3. Semi-supervised two-class clustering using GEBS.

where x_{ij} is the j^{th} feature for i^{th} pixel. $\mathbf{P}_B$ is similarly defined. The matrix of displacement vectors $\mathbf{Y}$ consists of $\vec{Y}_F$ with values +1 for the foreground seed points and $\vec{Y}_B$ with values -1 for the background seed points,

$$\mathbf{Y} = \begin{bmatrix} \vec{Y_F} & \vec{Y_B} & \vec{O} \end{bmatrix}^T \tag{14}$$

with

$$\vec{Y_F} = \left[\vec{d_1}^T \dots \vec{d_f}^T\right], \vec{Y}_B = \left[\vec{d_1}^T \dots \vec{d_b}^T\right]$$
$$\vec{d_i} = \begin{bmatrix} \pm 1 & \pm 1 & \pm 1 \end{bmatrix}^T \tag{15}$$

where $\vec{O}$ is a vector of zeros and $\vec{d_i}$ is a vector of +1 (-1) for the foreground (background) pixels. Once the displacement function (1) is learned (that is, by solving (8)) using interactively labeled pixel samples in a supervised manner, the GEBS classifier can be estimated and used to interpolate the labels of unlabeled pixels in the image. For classification purposes we use zero (midpoint value between -1 and $+1$) to threshold the vector $\vec{d}(\vec{x})$ and assign label $\ell(\vec{x})$ to a pixel by taking consensus among vector elements of $\vec{d}(\vec{x})$,

$$\ell(\vec{x}) = \begin{cases} foreground, \text{if majority } \vec{d}(\vec{x}) \text{ elements} \geq 0 \\ background, \text{if majority } \vec{d}(\vec{x}) \text{ elements} < 0. \end{cases} \tag{16}$$

3. EXPERIMENTAL RESULTS

In all our experiments reported here, we fixed the values of parameters ν and σ in Eq. (5) at 0.25 and 1 respectively. Experimental results also showed that final results were not affected by small variation in parameters values. We note that the parameter σ is used to control the spatial influence of the GEBS function which can be adjusted to optimize figure-ground separation. No pre-processing or post processing operations were performed on the GEBS segmentation results. The experiments were performed on a Windows laptop with 2.4GHz CPU, 2Gb RAM and MATLAB R2012a. For an image of size 321×481 pixels our GEBS scheme takes around 100 seconds after the initial seeds are selected.

Figure 2 shows some example segmentation results on natural images taken from the new Berkeley Segmentation Data Set (BSDS 500) [24] using our GEBS (Figure 2(c)) and the thin plate spline (TPS) regression method [8] (Figure 2(d)) along with one of the human annotated segmentations (Figure 2(b)) which serves as ground truth. To compare performance between the two algorithms we use the same user supplied sparse seed points in each case. As can be seen, our method clearly outperforms TPS based image segmentation without any leakages; see for example bottom two rows in Figure 2(d). It is also interesting to note that our GEBS scheme obtains better foreground segmentation even in the case of a sparse sample of seed points, see Figure 2 first row. We applied the GEBS approach for semi-supervised clustering as another application of user-defined seed points-based region partitioning. Figure 3 shows two-class clusters of varying shape, size, intensity and density, and the corresponding GEBS results. As can be seen we obtain a clear separation of clusters using sparse input from the user.

4. CONCLUSIONS

We have presented a novel adaptation of Gaussian elastic body splines (GEBS) for interactive image segmentation. It uses the strength of elastic body splines to learn an interpolating pixel classifier function that can be flexibly used for complex image segmentation tasks requiring manual supervision. The GEBS image segmentation is on-line, fast and easy to implement for grayscale images. Qualitatively the proposed GEBS method outperforms the thin-plate spline approach for pixel labeling. One of the main reasons for the improved performance is that the GEBS approach needs very few seed points to learn the pixel classification function while thin-plate splines are much more sensitive to the number of training samples.

5. ACKNOWELDGMENTS

This research was partially supported by U.S. Air Force Research Laboratory (AFRL) under agreement AFRL FA8750-14-2-0072. The views and conclusions contained in this document are those of the authors and should not be interpreted as representing the official policies, either expressed or implied, of AFRL or the U.S. Government.

6. REFERENCES

[1] J. Kohlrausch, K. Rohr, and H. Siegfried Stiehl, "A new class of elastic body splines for nonrigid registration of medical images," *Journal of Mathematical Imaging and Vision*, vol. 23, no. 3, pp. 253–280, 2005.

[2] E. N. Mortensen and W. A. Barrett, "Intelligent scissors for image composition," in *Proc. 22nd Annual Conference on Computer Graphics and Interactive Techniques*, 1995, pp. 191–198.

[3] A. X. Falcao and J. K. Udupa, "A 3D generalization of user-steered live-wire segmentation," *Medical Image Analysis*, vol. 4, no. 4, pp. 389–402, 2000.

[4] M. Kass, A. Witkin, and D. Terzopoulos, "Snakes: Active contour models," *International Journal of Computer Vision*, vol. 1, no. 4, pp. 321–331, 1988.

[5] V. Caselles, R. Kimmel, and G. Sapiro, "Geodesic active contours," *International Journal of Computer Vision*, vol. 22, no. 1, pp. 61–79, 1997.

[6] C. Rother, V. Kolmogorov, and A. Blake, "Grabcut: interactive foreground extraction using iterated graph cuts," *ACM Transactions on Graphics*, vol. 23, no. 3, pp. 309–314, 2004.

[7] L. Grady, "Random walks for image segmentation," *IEEE Transactions on Pattern Analysis and Machine Intelligence*, vol. 28, no. 11, pp. 1768–1783, 2006.

[8] S. Xiang, F. Nie, C. Zhang, and C. Zhang, "Interactive natural image segmentation via spline regression," *IEEE Transactions on Image Processing*, vol. 18, no. 7, pp. 1623–1632, 2009.

[9] T. F. Chan and L. Vese, "Active contours without edges," *IEEE Transactions on Image Processing*, vol. 10, no. 2, pp. 266–277, 2001.

[10] Y. Y. Boykov and M. P. Jolly, "Interactive graph cuts for optimal boundary & region segmentation of objects in N-D images," in *Proc. International Conference on Computer Vision (ICCV)*, 2001, vol. 1, pp. 105–112.

[11] V. Gulshan, C. Rother, A. Criminisi, A. Blake, and A. Zisserman, "Geodesic star convexity for interactive image segmentation," in *IEEE Conf. Computer Vision and Pattern Recognition*. 2010, pp. 3129–3136, IEEE.

[12] V. B. S. Prasath, F. Bunyak, P. Dale, S. R. Frazier, and K. Palaniappan, "Segmentation of breast cancer tissue microarrays for computer-aided diagnosis in pathology," in *IEEE Healthcare Innovation Conference*, 2012.

[13] K. Palaniappan, R. Rao, and G. Seetharaman, "Wide-area persistent airborne video: Architecture and challenges," in *Distributed Video Sensor Networks: Research Challenges and Future Directions*, pp. 349–371. Springer, 2011.

[14] A. Hafiane, F. Bunyak, and K. Palaniappan, "Evaluation of level set-based histology image segmentation using geometric region criteria," in *IEEE Int. Symposium Biomedical Imaging: From Nano to Macro*, 2009.

[15] F. Bunyak and K. Palaniappan, "Efficient segmentation using feature-based graph partitioning active contours," in *IEEE Int. Conf. Computer Vision*, 2009, pp. 873–880.

[16] J. Fraser, A. Haridas, G. Seetharaman, R. Rao, and K. Palaniappan, "Kolam: A cross-platform architecture for scalable visualization and tracking in wide-area motion imagery," in *Proc. SPIE Conf. Geospatial InfoFusion III*, 2013, vol. 8747, p. 87470N.

[17] A. Haridas, R. Pelapur, J. Fraser, F. Bunyak, and K. Palaniappan, "Visualization of automated and manual trajectories in wide-area motion imagery," in *15th Int. Conf. Information Visualization*, 2011, pp. 288–293.

[18] Y. Li, J. Sun, C. K. Tang, and H. Y. Shum, "Lazy snapping," *ACM Transactions on Graphics*, vol. 23, no. 3, pp. 303–308, 2004.

[19] J. He, C.-S. Kim, and C.-C. Jay Kuo, *Interactive Segmentation Techniques: Algorithms and Performance Evaluation*, Springer Briefs, 2014.

[20] M. H. Davis, A. Khotanzad, D. P. Flamig, and S. E. Harms, "A physics-based coordinate transformation for 3-D image matching," *IEEE Transactions on Medical Imaging*, vol. 16, no. 3, pp. 317–328, 1997.

[21] G. Seetharaman, G. Gasperas, and K. Palaniappan, "A piecewise affine model for image registration in nonrigid motion analysis," in *IEEE Int. Conf. Image Processing*, 2000, vol. 1, pp. 561–564.

[22] K. Palaniappan, H. S. Jiang, and T. I. Baskin, "Nonrigid motion estimation using the robust tensor method," in *IEEE CVPR Workshop on Articulated and Nonrigid Motion*, 2004, vol. 1, pp. 25–33.

[23] P. C. Chou and N. J. Pagano, *Elasticity: Tensor, Dyadic, and Engineering Approaches*, Dover Publications, 1992.

[24] P. Arbelaez, M. Maire, C. Fowlkes, and J. Malik, "Contour detection and hierarchical image segmentation," *IEEE Transactions on Pattern Analysis and Machine Intelligence*, vol. 33, no. 5, pp. 898–916, 2011.